*Article*

# Functional Coupling of the Locus Coeruleus Is Linked to Successful Cognitive Control

**Marcus Grueschow** [1,*], **Birgit Kleim** [2,3] **and Christian Carl Ruff** [1]

1 Zurich Center for Neuroeconomics (ZNE), Department of Economics, University of Zurich, 8006 Zurich, Switzerland; christian.ruff@econ.uzh.ch
2 Department of Experimental Psychopathology and Psychotherapy, University of Zurich, 8050 Zurich, Switzerland; b.kleim@psychologie.uzh.ch
3 Department of Psychiatry, Psychotherapy and Psychosomatics, University of Zurich, 8032 Zurich, Switzerland
* Correspondence: marcus.grueschow@econ.uzh.ch

**Abstract:** The locus coeruleus (LC) is a brainstem structure that sends widespread efferent projections throughout the mammalian brain. The LC constitutes the major source of noradrenaline (NE), a modulatory neurotransmitter that is crucial for fundamental brain functions such as arousal, attention, and cognitive control. This role of the LC-NE is traditionally not believed to reflect functional influences on the frontoparietal network or the striatum, but recent advances in chemogenetic manipulations of the rodent brain have challenged this notion. However, demonstrations of LC-NE functional connectivity with these areas in the human brain are surprisingly sparse. Here, we close this gap. Using an established emotional stroop task, we directly compared trials requiring response conflict control with trials that did not require this, but were matched for visual stimulus properties, response modality, and controlled for pupil dilation differences across both trial types. We found that LC-NE functional coupling with the parietal cortex and regions of the striatum is substantially enhanced during trials requiring response conflict control. Crucially, the strength of this functional coupling was directly related to individual reaction time differences incurred by conflict resolution. Our data concur with recent rodent findings and highlight the importance of converging evidence between human and nonhuman neurophysiology to further understand the neural systems supporting adaptive and maladaptive behavior in health and disease.

**Keywords:** response conflict; executive function; arousal; functional connectivity; parietal cortex; ventral striatum; dorsal striatum

## 1. Introduction

The locus coeruleus (LC) is a brainstem structure that sends widespread efferent projections to many regions in the mammalian brain [1,2]. The LC is the main source of the neurotransmitter noradrenaline (NE), which is essential for neuromodulation underlying the effects of arousal, attention, and cognitive control [3–7]. Specifically, LC-NE is thought to be important for the type of cognitive control that flexibly adapts cognition and action in line with internal goals or external task demands [8]. An important aspect of this is response conflict resolution, which is critical during decision making and adaptive behavior [9,10]. Response conflict emerges when a prepotent habitual response must be withheld in order to decide for an alternative option that better suits the current behavioral aims or rules [8,11]. There is considerable variability in the capacity to resolve response conflict between individuals, but the neural origins of heterogeneity in this important aspect of adaptive behavior (and its potential links to the LC-NE system) are currently not well understood.

A prominent model of cognitive control postulates that the current level of behavioral conflict must first be registered and monitored [12–15] before this information is communicated to regions that subsequently implement appropriate adjustments and resolve the

conflict through cortical amplification of task relevant information [8,16,17]. It is typically assumed that the preferential processing of relevant information is supported by a distributed network that includes frontal and parietal cortical structures [18,19]. Interestingly, such selective information processing in frontoparietal networks has been proposed to depend on the release of neuromodulators from subcortical areas [7,20–23], in particular from the LC-NE noradrenergic system [5,7,24,25]. More specifically, previous work has outlined that the activation of the noradrenergic system increases the signal to noise ratio of currently relevant representations and biases the competition for processing resources across multiple levels of the cortical hierarchy [24–26]. However, while research on the human noradrenergic system is increasing [27–33], direct investigations of LC-NE involvement in adaptive behavior, such as cognitive control and selective attention, is scarce [34–37]. Specifically, the functional connectivity of the LC-NE and its specific behavioral relevance is a particularly understudied area of research in humans [34,36].

Neurophysiological research on rodents and nonhuman primates has identified the LC-NE as the center of the mammalian arousal system [25,38–40] and as being important for determining levels of wakefulness [41–43]. In contrast, the LC-NE has largely been regarded as unable to modulate activity in attention relevant specific cortical networks [5]. However, recent studies [44] have proposed that the LC-NE neuromodulatory system may be capable of biasing the processing of task relevant information via thalamocortical and midbrain circuits [5,26]. Specifically, recent advances in optogenetic and chemogenetic manipulation of the rodent brain have revealed novel insights into this function and the connectivity of the LC-NE arousal system [44,45]. For instance, chemogenetically activating the rodent LC-NE leads to rapid reconfigurations of resting state connectivity in multiple networks, including the fronto-parietal network as well as a striato-motor network [44]. Moreover, artificially increasing LC-NE firing in this study also revealed strong noradrenergic innervation and increased NE turnover in the dorsal striatum (caudate nucleus), even though this region is widely thought to lack any NE projections [25,46–49]. However, it has to be noted that early neurophysiological studies in mice have revealed that the shell of the ventral striatum (nucleus accumbens) has a high number of LC projections [50,51]. Importantly, while these animal studies reveal crucial insights into the connectivity architecture of the LC-NE neuromulatory system, they are largely conducted under some form of anesthesia, leaving it unclear to what degree these connections are behaviorally relevant and whether similar connectivity patterns would also arise in humans. Here, we investigate the functional connectivity of the human LC-NE with these cortical and subcortical structures and investigate their behavioral relevance during an important aspect of adaptive behavior: response conflict resolution.

We focused on response conflict resolution because theoretical work has speculated that it may be closely linked to noradrenergic arousal processes and the functioning of the LC-NE arousal system [6,52,53]. Recent studies have, indeed, provided behavioral and pupillometry (a potential proxy for LC-NE firing [44,54–59]) evidence for this link [60,61]. In addition, human neurophysiological data link the LC-NE arousal system to individual differences in conflict resolution [34–37], but its specific functional contributions are not well understood (see below). Classic cognitive control tasks—such as, for example, the flanker task, the color–word stroop task or the emotional stroop task, which we use here—employ reaction times to quantify the individual's capacity for conflict resolution [8,12,13]. More specifically, a longer reaction time for conflict trials (requiring conflict resolution) compared to no conflict trials (requiring no conflict resolution) is thought to reflect that conflict resolution incurs processing costs involving detection, monitoring and, eventually, adjusting to the behavioral conflict [8,12]. One dominant account posits that this reaction time increase is smaller for individuals with better capacity to resolve the behavioral conflict, as we have found in a previous analysis of these data [34], that, however, has not investigated the individual relationship of reaction times and behavioral accuracy. Therefore, an alternative account suggests that individuals generally aim to maximize task-performance and employ a speed–accuracy trade-off during conflict resolution, which

produces individually increased task-performance with longer reaction times for better conflict resolution [62–64]. However, several lines of research have also suggested a role of the LC-NE in response inhibition, implicating that LC-NE activity may relate to longer RTs and reduced impulsivity [65–69]. Here, we test these accounts, by relating individual differences in reaction time induced by conflict resolution to individual differences in choice accuracy. Moreover, we relate these indices to the functional coupling of the LC-NE arousal system, to test the hypothesis derived from animal neurophysiological studies that the LC-NE may enhance its functional coupling with regions of the fronto-parietal network known to be involved in selective attention. In addition we explore whether the connectivity between LC-NE and subcortical areas, such as the dorsal and ventral striatum, previously reported in rodents [44], can also be observed in humans and whether LC-NE connectivity to these areas is related to the efficiency of behavioral conflict resolution.

## 2. Material and Methods

### 2.1. Participants

Forty-eight medical students ($n$ = 28 women, mean age = 24 years, $SD$ = 1.99) were recruited using standard exclusion criteria (fMRI safety, psychopathology). Written informed consent was provided by each participant. Participation was voluntary. Participants were debriefed and compensated (equal to 35 US$). The Cantonal Ethics Committee of Zurich (KEK) approved all procedures prior to study commencement. The results presented here are an addendum analysis to a prior publication using this data set [34], which reported the functional connectivity of the dorso-medial prefrontal cortex (DMPFC), not the locus coeruleus.

### 2.2. Stimulus Presentation

All stimuli were displayed on a grey projection screen (using the Cogent2000-toolbox, http://www.vislab.ucl.ac.uk/cogent_2000.php, accessed on 11 April 2017, implemented in Matlab, The MathWorks, Inc., Natick, MA, USA) which participants viewed by means of a mirror system mounted atop the MR head coil. The vast majority of participants (46 out of 48) completed two runs (200 trials) of the emotional stroop task (see below), while two participants only conducted one run (100 trials). To optimally spread 100 trials across the 10 min of one functional run time, the intertrial intervals (ITI) for each participant were individually sampled from a gamma distribution using the matlab function gamrnd.m (Matlab, Mathworks) with shape parameter 2 and scale parameter 1 and truncated within 2 and 6 s, yielding a mean ITI of 3.1 s.

### 2.3. Behavioral Task

To induce trials with and without response conflict, we used the emotional stroop task [70–72], a wellestablished laboratory procedure involving response conflict [73,74]. The participants task was to categorize faces with respect to their emotional expression (happy vs. fearful). Critically, at the same time, participants had to ignore overlayed emotionally congruent I or incongruent (I) words ("HAPPY", "FEAR", Figure 1A,B). The induced processing costs during conflict typically induce higher reaction times (RT) for incongruent than congruent trials [70,71,75] (Figure 1C–F).

The task sequence consisted of fifty no conflict trials (congruent) and fifty conflict trials (incongruent). The varying face/word stimulus combination were shown in pseudorandom order. In addition, the different stimulus categories were counterbalanced for equal numbers of congruent–congruent, congruent–incongruent, incongruent–congruent, and incongruent–incongruent temporal stimulus order (but in the present work we focus on congruency effects only; the trial wise sequence effects along with a more detailed description of the task design are described elsewhere [35]). The participants' task was to respond as quickly and accurately as possible to the emotionality of the face (press left button for a happy face, press right button for fear or vice versa).
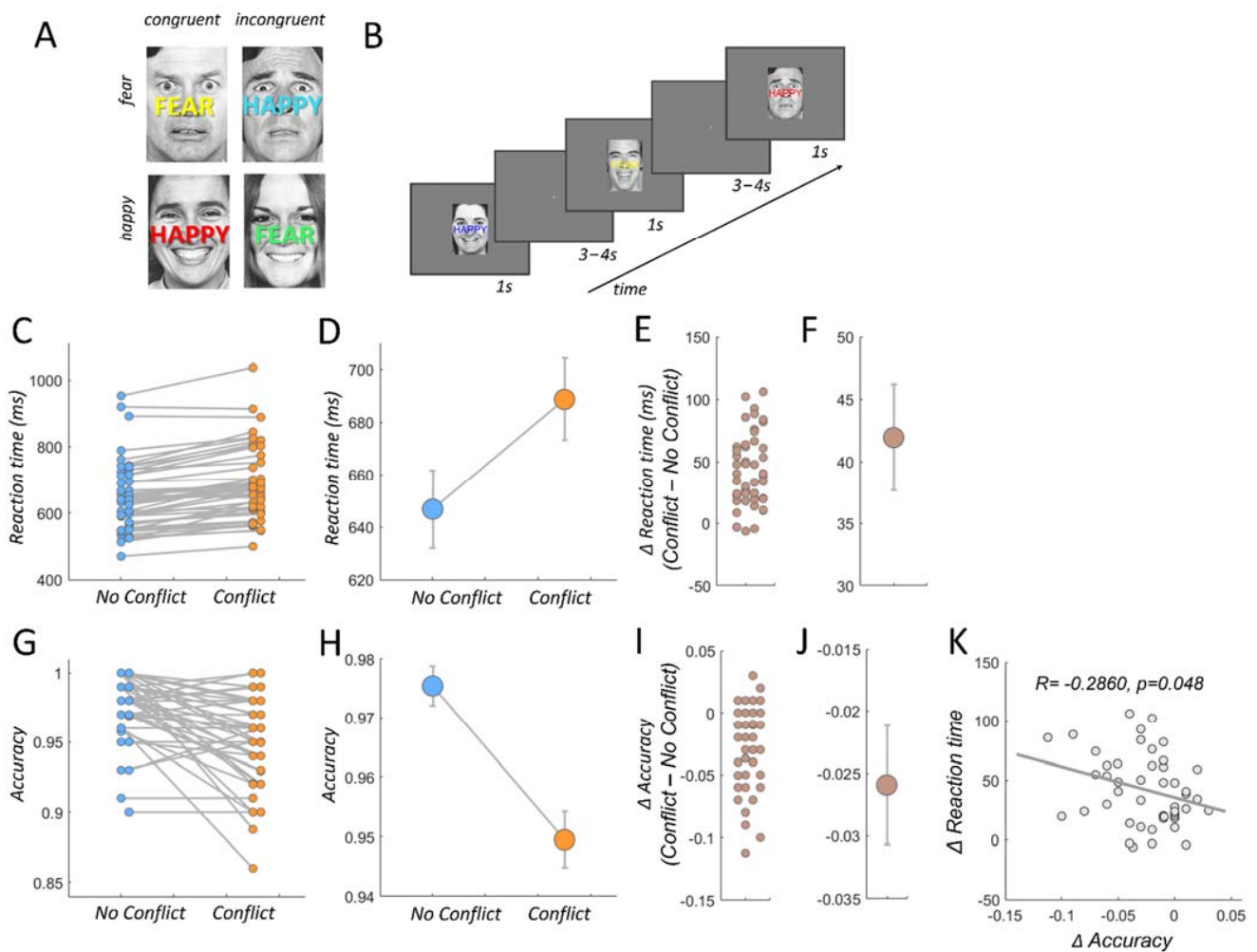
**Figure 1.** Experimental paradigm and behavioral results. (**A**) The emotional stroop task consists of four possible face/word combinations. Participants identify the emotion of the face and ignore the overlaid word. Adaptation effects were minimized by varying the word color randomly with every trial. (**B**) Trial order presentation example. (**C**) Individual reaction times in congruent (no conflict) and incongruent trials (conflict). (**D**) Mean reaction times in congruent (no conflict) and incongruent trials (conflict). Error bars represent $\pm 1$ standard error of the mean (SEM). (**E**) Individual reaction time differences between no conflict and conflict trials. (**F**) Mean reaction times are significantly increased in conflict versus no conflict trials ($T_{47} = 9.88$, $p = 4.67 \times 10^{-13}$). Error bars represent $\pm 1$ standard error of the mean (SEM). (**G**) Individual response accuracy in no conflict and conflict trials. (**H**) Mean response accuracy in no conflict and conflict trials. Error bars represent $\pm 1$ standard error of the mean (SEM). (**I**) Individual response accuracy differences between no conflict and conflict trials. (**J**) Mean response accuracy is significantly decreased in conflict versus no conflict trials ($T_{47} = -5.25$, $p = 3.65 \times 10^{-6}$). Error bars represent $\pm 1$ standard error of the mean (SEM). (**K**) Individual conflict related reaction time increases are negatively correlated with the individual conflict related decreases in response accuracy ($p = 0.0488$, R $= -0.2860$).

## 2.4. Behavioral Analyses

We acquired reaction times and accuracy rate, which is defined as the proportion of trials with correct identification of the emotional valence of the face expression. We excluded trials with RTs exceeding two standard deviations from the mean (across all trials). These trials entered the fMRI model as trials of no interest [70,71,76] (see below). Correlations between behavioral measures and comparison between conflict (I) vs. no conflict trial (C) were conducted via Pearson correlation coefficient and paired t-tests, respectively, implemented in the statistics toolbox in matlab. The mean reaction time

difference between congruent and incongruent trials (Figure 1E) served as an individual score for response conflict resolution and was regressed against individual functional connectivity difference between these trial types (Figure 2D,E).
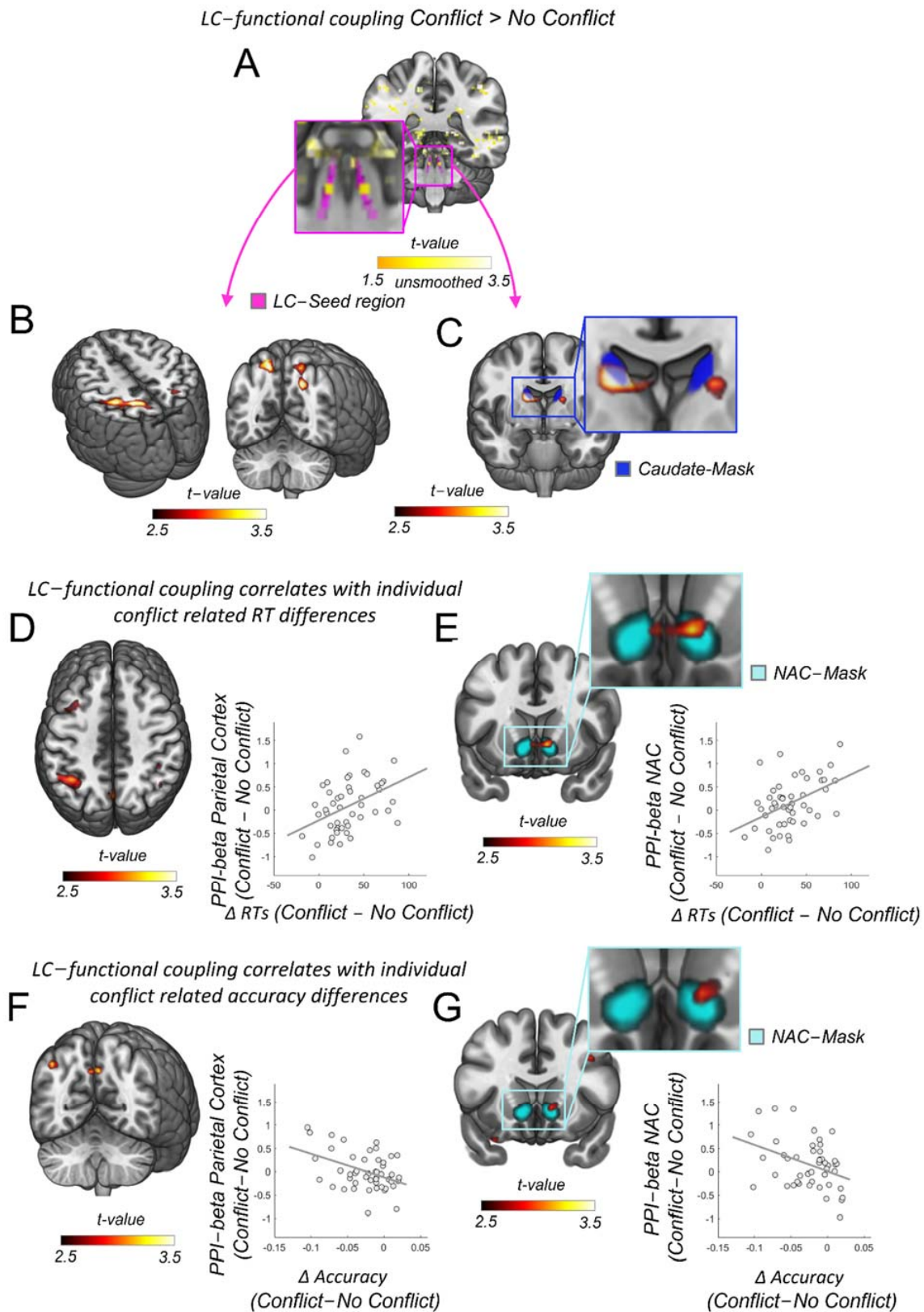


**Figure 2.** LC functional connectivity to parietal cortex and nucleus accumbens relates to individual differences in reaction times during cognitive control. (**A**) Enhanced activity during conflict versus

no conflict trials precisely within the LC-NE 1SD-mask from Keren et al., 2009 (in magenta [77]). Yellow color scale represents the uncorrected average across unsmoothed-physio-corrected I > C individual contrast maps (LC-left: T = 1.77, $p$ = 0.41, X/Y/Z: $-5/-37/-25$, LC-right: T = 1.77, $p$ = 0.41, X/Y/Z: $-6/-37/-25$, N = 48). (**B**) Increased functional coupling between LC-NE and parietal cortex in conflict versus no conflict trials (family wise error corrected), $T_{(FWE)}$ = 5.33, $P_{(FWE)}$ = 0.005, X/Y/Z: $-30/-42/48$, k = 149). (**C**) Increased functional coupling between LC-NE and the dorsal striatum in conflict versus no conflict trials (small volume peak corrected (SVC) in the bilateral caudate nucleus, $T_{(SVC)}$ = 4.37, $P_{(SVC)}$ = 0.008, $13/-5/18$). Caudate nucleus mask in blue. (**D**) Individual increases in LC-NE functional connectivity to the parietal cortex due to conflict correlate with individual conflict-related reaction timeIcrIes (FWE), $I_{(FWE)}$ = 4.14, $P_{(FWE)}$ = 0.018, X/Y/Z: $-40/-55/48$. For visualization purposes: the correlation between the response conflict resolution score in reaction time and the functional coupling between the LC-NE and the peak voxel in the parietal cortex (voxel coordinates at X/Y/Z: $-40/-55/48$, N = 48). (**E**) Individual increases in LC-NE functional connectivity to the ventral striatum due to conflict correlate with individual conflict related reaction time increases (small volume peak corrected (SVC) in the bilateral nucleus accumbens, $T_{(SVC)}$ = 3.87, $P_{(SVC)}$ = 0.021, $11/1/-10$). For visualization purposes: the correlation between the response conflict resolution score in reaction time and the functional coupling between the LC-NE and the peak voxel in the nucleus accumbens (voxel coordinates at X/Y/Z: $11/1/-10$, N = 48). (**F**) Individual increases in LC-NE functional connectivity to the parietal cortex due to conflict correlate with individual conflict related accuracy decreases at trend level (uncorrected, $T_{(uncorr)}$ = 3.16, $P_{(uncorr)}$ = 0.001, X/Y/Z: $-35/-75/28$). For visualization purposes: the correlation between the accuracy differences and the functional coupling between the LC-NE and the peak voxel in the parietal cortex (voxel coordinates at X/Y/Z: $-35/-75/28$, N = 48). (**G**) Individual increases in LC-NE functional connectivity to the ventral striatum due to conflict correlate with individual conflict related accuracy decreases at trend level (uncorrected, $T_{(uncorr)}$ = 2.71, $P_{(uncorr)}$ = 0.005, $11/18/-5$). For visualization purposes: the correlation between the accuracy differences and the functional coupling between the LC-NE and the peak voxel in the nucleus accumbens (voxel coordinates at X/Y/Z: $11/18/-5$, N = 48).

### 2.5. The fMRI Image Acquisition

Our participants performed two 9.75 min functional imaging sessions during which they performed the emotional stroop task. Per each session, 225 T2* weighted whole brain echo planar images were acquired via a Philips Achieva 3 T whole body scanner (Philips Medical Systems, Best, The Netherlands) and an 8-channel Philips sensitivity encoded (SENSE) head coil (imaging parameters: 2600 ms repetition time (TR); 40 ms (TE); 37 slices (transversal, ascending acquisition); 2.6 mm slice thickness; 2.5 mm × 2.5 mm in plane resolution; 0.65 mm gap; 90° flip angle). Five dummy scans were obtained and discarded before functional image acquisition started to measure at fully equilibrated magnetic field. Additionally, a high resolution T1-weighted 3D fast field echo anatomical scan was acquired for better registration to MNI standard space (sequence parameters: 181 sagittal slices; matrix size: 256 × 256; voxel size: 1 × 1 × 1 mm; TR/TE/TI: 8.3/2.26/181 ms).

### 2.6. The fMRI Image Preprocessing

For image preprocessing and statistical analysis, we employed SPM12 (Wellcome Trust Centre for Neuroimaging). Each functional image was slice–time corrected using the middle slice acquisition time as reference. Participants' head motion was accounted for using standard SPM12 realignment procedures. Each individual T1-weighted anatomical scan was coregistered to the mean functional image and normalized to the standard T1-MNI template using the "Unified Segment" procedure, as implemented by SPM12 [78]. We normalized the functional images to the MNI standard brain template with the same transformation. Finally, we spatially resampled to 2.5 mm isotropic voxels, and smoothed the resulting images with a Gaussian kernel (FWHM, 6 mm).

### *2.7. The fMRI Data Analysis*

First, a general linear model (GLM) was defined containing the main effects, such as conflict and no conflict trials, to serve as a base model with which we control for these main effects, in order to be able to make unconfounded inference on the psychophysiological interaction (PPI) term indicating functional coupling (see below). The base GLM contained two indicator functions at the onset of each of the two trial types (congruent and incongruent). Trials of no interest (see above) were modelled with an additional indicator function [70,71]. For each voxel the BOLD signal was regressed on these conditions with a standard set of hyperparameters modelling MR image autocorrelations with a first order autoregressive model. Head motion was accounted for with additional regressors of no interest constituting six motion parameters which were obtained during the realignment procedure. Moreover, we also accounted for potential confounding effects of eye movements, blinks and pupil size by including these measures in our GLM. Controlling for pupil size in this analysis aimed at counteracting any potential impact that average visual light reflections may have on activity throughout the brain. We employed an MR compatible infrared EyeLink II CL v4.51 eye tracker system (SR Research Ltd., Ottawa, ON, Canada) to sample the eye related information at 500Hz during functional image acquisition. We defined saccades as eye movements extending 0.5 degrees visual angle [79] and eye blinks as periods of signal loss between 80–2000ms [80]; we accounted for these signal losses by linear interpolation [81]. The regressors for saccades and pupil also contained a parametric modulation of eye movement distance and pupil size, respectively.

Imaging the LC-NE in the brainstem is difficult because of its small size and the surrounding ventricles. Low signal to noise ratio in the brainstem is due to breathing and pulsating artifacts [82]. For that reason, we additionally accounted for physiological noise using nuisance regressors that reflected the time-course of signals in the cerebrospinal fluid (CSF) [83]. To this end, we made use of the individual CSF mask that was created during the nonlinear unified segment procedure in SPM12 (see above). For every voxel within this CSF mask, we extracted the BOLD time series and applied a principal component analysis by means of the matlab function pca.m, which is part of the statistics toolbox (MATLAB, The MathWorks, Inc., Natick, MA, USA, version 2017a). The first five principal components were then entered as additional nuisance regressors in the GLM analysis, to account for physiological noise. This procedure has been successfully applied previously and shown to substantially increase signal to noise ratio in the brainstem [35,83]. Statistical inference was drawn via a random effects General Linear Model using the SPM12 framework. We adIed a whole brain FWE-corrected statistical threshold of $p < 0.05$ with an initial cluster-forming voxel level threshold of T = 3.275 (corresponding to uncorrected $p < 0.001$) [84]. For our hypothesis guided ROI analysis investigating LC-NE functional coupling with dorsal and ventral striatum, we employed a standard small volume peak level correction restricted to a caudate nucleus mask provided by the NITRC Atlas of the basal ganglia (https://www.nitrc.org/projects/atag/, accessed on 23 November 2019) and the nucleus accumbens mask provided by the FSL-Harvard-Oxford-atlas (http://neuro.debian.net/pkgs/fsl-harvard-oxford-atlases.html, accessed on 6 November 2013).

### *2.8. Psychophysiological Analysis (PPI)*

To investigate the functional coupling of the LC-NE we used a standard PPI approach as implemented in SPM 12, which adds to the base GLM design matrix that includes the main effects of the task the BOLD time series extracted from a 3mm sphere centered on the peak activity identified with the incongruent > congruent contrast within the standard LC-NE mask (1SD mask from Keren et al. [77], Figure 2A). In addition, we added two interaction terms which reflect the interactions of the extracted LC-NE BOLD time course with the C and I regressors. It is important to note that these PPI interaction terms are not confounded with the main effects and interactions with all other experimental variables because they are part of the base GLM design matrix along with physiological, pupil and eye-tracking data (see above) and, thus, accounted for.

The full list of regressors finally included: 'congruent trials', 'incongruent trials', 'trials of no interest', 'blinks', 'saccades', 'pupil size', 'congruent trials PPI', 'incongruent trials PPI', '6 motion regressors' and '5 physiological noise regressors'. To assess the relationship between conflict related functional coupling and behavioral measures, we correlated the size of the functional coupling difference (I > C) with equivalent behavioral differences in reaction time (RT difference between I > C) and accuracy differences between both trial types (I > C) (Figure 1) in a second level analysis. For brain visualizations (Figure 2), we used the freely available software MRIcroGL (https://www.nitrc.org/projects/mricrogl/, accessed on 2 November 2017).

## 3. Results

### 3.1. Behavioral Results

We replicate and confirm previous effects of response conflict resolution for RTs and accuracy [13,70,85]. As expected, responses to trials requiring conflict resolution (incongruent trials) took more time [75]. A comparison between incongruent (conflict) and congruent (no conflict) trials revealed significantly increased reaction times ($T_{47} = 9.88$, $p = 4.67 \times 10^{-13}$, Figure 1C–F) and decreased accuracies ($T_{47} = -5.25$, $p = 3.65 \times 10^{-6}$, Figure 1G–J), and these two behavioral indices of response conflict were negatively correlated ($p = 0.0488$, R = −0.2860, Figure 1K). In other words, the longer an individual takes, on average, to resolve the conflict, the lower the response accuracy during conflict, speaking against a speed accuracy trade-off. In the next analyses, we identified regions with which the LC-NE showed stronger functional coupling during conflict as compared to no conflict trials. In addition, we looked for regions whose functional coupling strength with the LC-NE reflected the individual conflict related enhancement in RTs, indicating that these functional connections are relevant for efficient conflict resolution.

### 3.2. LC Functional Coupling Relates to Individual RTs during Conflict Resolution

The resolution of conflict incurs processing costs due to detection, monitoring, and, eventually, adjusting the behavioral conflict. These processes require preferential processing of task relevant information, which is thought to be supported by the fronto-parietal network [18,19]. In addition, it has been suggested that such selective information processing in the fronto-parietal networks depends on the release of neuromodulators from subcortical areas [7,20–23] and, especially, the noradrenergic system [5,7,24,25]. Our results are congruent with such an account: We first found that the LC-NE shows enhanced activity during conflict versus no conflict trials. As recommended for brainstem imaging [86], we employed the uncorrected average across unsmoothed and physiological noise corrected individual I > C contrast maps (LC-left: T = 1.77, $p = 0.41$, X/Y/Z: −5/−37/−25, LC-right: T = 1.77, $p = 0.41$, X/Y/Z: −6/−37/−25, N = 48, Figure 2A). Secondly, we find significantly enhanced functional coupling between the LC-NE arousal system and the fronto-parietal brain network during conflict trials as compared to no conflict trials, in particular, for clusters inIe parietaIortex (T$_{(FWE)}$ = 5.33, P$_{(FWE)}$ = 0.005, X/Y/Z: −30/−42/48, Figure 2B). The level of enhanced functional coupling between the LC-NE and the parietal cortex due to conflict resolution was correlated with the individual cIliI related Iincrease (FWE), T$_{(FWE)}$ = 4.14, P$_{(FWE)}$ = 0.018, X/Y/Z: −40/−55/48, Figure 2D), indicating a strong behavioral relevance for these connections during response conflict adjustment. Similar functional connectivity patterns were also found for regions in the dorsal and ventral striatum, even though these regions have been thought to be devoid of any noradrenergic innervations [25,46–49]. Specifically, LC-NE functional coupling in conflict versus no conflict trials was substantially enhanced in the caudate nucleus in the dorsal striatum (small volume peak corrected (SVC) in the bilateral caudate nucleus, T$_{(SVC)}$ = 4.37, P$_{(SVC)}$ = 0.008, 13/−5/18, Figure 2C), and the level of enhanced functional coupling between the LC-NE and the ventral striatum, particularly the nucleus accumbens, due to conflict resolution was correlated with the individual conflict related RT increase (small volume peak corrected (SVC) in the bilateral nucleus accumbens, T$_{(SVC)}$ = 3.87, P$_{(SVC)}$ = 0.021, 11/1/−10,

Figure 2E). As we observed that conflict induced response slowing and accuracy changes were correlated (Figure 1K), we also tested whether LC-NE functional coupling strength would relate to corresponding changes in accuracy. We, indeed, found such correlations in parietal and striatal regions, but only at an uncorrected trend level (Figure 2F,G). Specifically, the LC functional coupling strength in regions of the parietal cortex and the ventral striatum correlated with the accuracy decreases for conflict versus no conflict trials (uncorrected, parietal cortex: $T_{(uncorr)} = 3.16$, $P_{(uncorr)} = 0.001$, X/Y/Z: $-35/-75/28$, ventral striatum, nucleus accumbens: $T_{(uncorr)} = 2.71$, $P_{(uncorr)} = 0.005$, $11/18/-5$, Figure 2F,G). Thus, our findings suggest a behavioral relevance of LC-NE coupling in response to conflict resolution, but no involvement in speed–accuracy trade-off (for which we should have seen positive correlations with both reaction time and accuracy increases). Nevertheless, these results suggest that functional connections between LC-NE and the parietal cortex and striatum are recruited during response conflict adjustments and play a functional role for such adaptive behavior.

## 4. Discussion

The resolution of response conflict is a crucial aspect in decision-making and a hallmark of adaptive behavior in animals and humans. The capacity for conflict resolution varies widely across individuals, while the neural origins of this heterogeneity remained elusive. Testing hypotheses derived from animal neurophysiology, we showed that behavioral variability in resolving response conflict in an emotional stroop task related to the functional coupling of the LC-NE arousal system with regions in the frontoparietal network as well as striatal regions. Our results reveal that the stronger the individual LC-NE functional coupling during conflict resolution with the parietal cortex and the nucleus accumbens, the longer the individuals take to resolve the conflict, and the less successful they are at it. While our data, thus, do not support a role for human LC-NE arousal system in implementing speed–accuracy trade-offs, they nevertheless reveal LC-NE involvement in response inhibition during cognitive control, which is more taxing in people who are worse at this cognitive function. These findings are not only relevant for future investigations of maladaptive cognitive control behavior, as prevalent in anxiety and depression, but also for disorders involving maladaptive impulse control behavior, such as addiction, obesity, or attention deficit hyperactivity disorder (ADHD) [87].

Several studies in rodents have previously indicated that fundamental behavioral functions such as sustained attention and response inhibition are modulated by the noradrenergic system [65–68]. For instance, previous studies have shown that increasing NE by blocking its reuptake in the forebrain enhances the animals' sustained attention and substantially improves response inhibition [65–69]. Interestingly, a recent study in mice showed that LC-NE stimulation increased goal directed attention and decreased impulsivity, while LC-NE suppression heightened distractibility and increased impulsive responding [21]. Moreover, in this study, LC-NE stimulation during the sustained attention task significantly enhanced attentional control, which led to decreasing premature responding, i.e., less impulsivity and, thus, longer reaction times. Similar effects could be observed in a prior study in healthy humans, which highlighted the selective involvement of NE in response inhibition [88]. More specifically, neurochemical inhibition of central noradrenaline reuptake specifically improved response inhibition but had no effect on probabilistic learning, whereas the inhibition of central serotonin reuptake impaired probabilistic learning with no effect on response inhibition [88]. These converging lines of research in animals and humans implicate the noradrenergic system in goal directed behavior and response inhibition, which is well in line with our findings of enhanced LC-NE connectivity during conflict resolution, during which response inhibition is paramount. More specifically, an essential behavioral part in response conflict resolution is to withhold the prepotent conflicting response until the conflict is solved and the alternative action (button press) can be initiated. To make an informed decision, sustained attention has to be employed to focus on task relevant information and filter out task irrelevant stimulus

features [19]. This preferential processing of relevant information incurs processing costs, supported by the fronto-parietal network, resulting in increased reaction times [18,19]. Our data show that the LC-NE functional coupling with the parietal cortex during conflict resolution is strongest for individuals who take longer, potentially resembling mice data where enhanced noradrenergic tone decreased impulsivity [65–69]. However, given our correlational approach, we cannot directly speak to the question of whether enhanced functional connectivity is also reflected in enhanced noradrenergic release from the LC-NE. Specifically, the PPI approach cannot logically identify whether any covariance in the residual fMRI timeseries reflects monosynaptic connectivity between two areas, or joint innervation by a third area, or trial-wise endogenous variation in some cognitive state that simultaneously affects both areas. Our PPI results, therefore, need to be interpreted along all these lines, since there is no principled way to rule out either of these effects.

In the influential conflict-monitoring framework of cognitive control, the dorso-medial prefrontal cortex (DMPFC) detects and monitors the level of behavioral conflict [12–15]. In this model, DMPFC communicates this information to the dorso-lateral prefrontal cortex (DLPFC), which constitutes an important part of the fronto-parietal network. The DLPFC is believed to be responsible for implementing appropriate adjustments via the cortical amplification of task relevant information and, thereby, helping the resolution of the conflict [8,16,17]. We have recently shown that the DMPFC also connects functionally to the LC-NE during conflict resolution [34] in humans. Similar results have been identified in animal tracing studies, which provided evidence for anatomical [89–91] and functional connections between the conflict monitoring DMPFC and the LC-NE [92–95]. This functional connection may serve as a potential source of information about the current level of conflict to the LC-NE and whether the modulation of parietal cortex is still required for response inhibition, while the processes of conflict resolution are still ongoing via sustained attention to task relevant information.

Until recently, it was unclear whether the LC-NE arousal system even innervates the fronto-parietal network [5] or projects to regions in the striatum [25,46–49]. Our data suggest a functional coupling between these regions also in humans. Novel insights into the connectivity of the LC-NE arousal system have been made specifically through recent advances in optogenetic and chemogenetic manipulation of the rodent brain [44,45]. More specifically, activating the LC-NE in mice via chemogenetic manipulation induced a massive and rapid reconfiguration of the resting state connectome [44]. These changes were observed in multiple networks, including the fronto-parietal but also the striato-motor-network, suggesting previously unknown noradrenergic innervation in these regions [25,46]. These conjectures were corroborated by this previous study, by its also finding an increased turnover of noradrenaline in the dorsal striatum after artificially increasing LC-NE firing [44]. Our data suggest similar functional connections also in humans, as we found LC-NE functional coupling between the parietal-cortex and with the dorsal and ventral striatum during response conflict resolution. Finding these connections during active behavior in humans and also establishing their behavioral relevance is important because most rodent studies are typically conducted under anesthesia, which precludes any inference on behavioral impact [44].

Our functional connectivity results of the LC-NE arousal system during cognitive control are also relevant for a number of psychiatric disorders with impairments of adaptive behavior and potential malfunctions of the noradrenergic system, such as anxiety, depression, addiction and PTSD [96–104]. For instance, it has been demonstrated that photostimulation of LC-NE projections to the amygdala caused noradrenaline release, which, in turn, resulted in anxiety like and aversive behavior in mice [99,105]. A recent human imaging study tested these observations using psychophysiological interaction analysis during cognitive control, as we have employed here, and showed that the functional connectivity between LC-NE and amygdala is a crucial predictor for increases in anxiety and depression symptoms after prolonged exposure to stress [35]. This example, and the current data, therefore showcase how hypotheses derived from animal neurophysiology can

inform human studies to test the functional and behavioral relevance of the neural arousal circuits [42]. The combination of novel connectivity methods [106–109] with behavioral tasks that drive the LC-NE [110–114], as well as the use of indirect measures of LC-NE activity such as pupil dilation and heart-rate variability [114–117], hold great promise to further our understanding of the LC-NE arousal system and its contribution to various psychopathologies [118–120].

## 5. Conclusions

In conclusion, we show that the level of functional coupling of the LC-NE arousal system with the parietal cortex and the striatum during cognitive control in humans is directly related to the individual differences in reaction times, supporting a role in response inhibition. These connectivity profiles are remarkable because it has been generally thought that the LC-NE does not innervate the frontoparietal or striatal regions. Our findings may also hold clinical relevance for psychopathologies with cognitive control impairments, such as anxiety, depression, addiction and PTSD.

## References

1. Manaye, K.F.; McIntire, D.D.; Mann, D.M.A.; German, D.C. Locus coeruleus cell loss in the aging human brain: A non-random process. *J. Comp. Neurol.* **1995**, *358*, 79–87. [CrossRef] [PubMed]
2. Sara, S.J.; Bouret, S. Orienting and Reorienting: The Locus Coeruleus Mediates Cognition through Arousal. *Neuron* **2012**, *76*, 130–141. [CrossRef] [PubMed]
3. Usher, M.; Cohen, J.D.; Servan-Schreiber, D.; Rajkowski, J.; Aston-Jones, G. The Role of Locus Coeruleus in the Regulation of Cognitive Performance. *Science* **1999**, *283*, 549–554. [CrossRef] [PubMed]
4. Uematsu, A.; Tan, B.Z.; Ycu, E.A.; Cuevas, J.S.; Koivumaa, J.; Junyent, F.; Kremer, E.; Witten, I.B.; Deisseroth, K.; Johansen, J.P. Modular organization of the brainstem noradrenaline system coordinates opposing learning states. *Nat. Neurosci.* **2017**, *20*, 1602–1611. [CrossRef] [PubMed]
5. Dahl, M.J.; Mather, M.; Werkle-Bergner, M. Noradrenergic modulation of rhythmic neural activity shapes selective attention. *Trends Cogn. Sci.* **2021**, *26*, 38–52. [CrossRef]
6. Verguts, T.; Notebaert, W. Adaptation by binding: A learning account of cognitive control. *Trends Cogn. Sci.* **2009**, *13*, 252–257. [CrossRef] [PubMed]
7. Thiele, A.; Bellgrove, M. Neuromodulation of Attention. *Neuron* **2018**, *97*, 769–785. [CrossRef]
8. Egner, T. *The Wiley Handbook of Cognitive Control*; Egner, T., Ed.; John Wiley & Sons Ltd.: Hoboken, NJ, USA, 2017.
9. Miller, E.K.; Cohen, J.D. An Integrative Theory of Prefrontal Cortex Function. *Annu. Rev. Neurosci.* **2001**, *24*, 167–202. [CrossRef]
10. Mansouri, F.A.; Tanaka, K.; Buckley, M.J. Conflict-induced behavioural adjustment: A clue to the executive functions of the prefrontal cortex. *Nat. Rev. Neurosci.* **2009**, *10*, 141–152. [CrossRef]
11. Stroop, J.R. Studies of interference in serial verbal reactions. *J. Exp. Psychol. Gen.* **1992**, *121*, 15–23. [CrossRef]
12. Botvinick, M.M.; Braver, T.S.; Barch, D.M.; Carter, C.S.; Cohen, J.D. Conflict monitoring and cognitive control. *Psychol. Rev.* **2001**, *108*, 624–652. [CrossRef] [PubMed]

13. Botvinick, M.M.; Cohen, J.D.; Carter, C.S. Conflict monitoring and anterior cingulate cortex: An update. *Trends Cogn. Sci.* **2004**, *8*, 539–546. [CrossRef]

14. Etkin, A.; Egner, T.; Kalisch, R. Emotional processing in anterior cingulate and medial prefrontal cortex. *Trends Cogn. Sci.* **2011**, *15*, 85–93. [CrossRef] [PubMed]

15. Critchley, H.D.; Mathias, C.J.; Josephs, O.; O'Doherty, J.; Zanini, S.; Dewar, B.; Cipolotti, L.; Shallice, T.; Dolan, R. Human cingulate cortex and autonomic control: Converging neuroimaging and clinical evidence. *Brain* **2003**, *126*, 2139–2152. [CrossRef]

16. Egner, T.; Hirsch, J. Cognitive control mechanisms resolve conflict through cortical amplification of task-relevant information. *Nat. Neurosci.* **2005**, *8*, 1784–1790. [CrossRef]

17. Ridderinkhof, K.R.; Wildenberg, W.P.V.D.; Segalowitz, S.J.; Carter, C.S. Neurocognitive mechanisms of cognitive control: The role of prefrontal cortex in action selection, response inhibition, performance monitoring, and reward-based learning. *Brain Cogn.* **2004**, *56*, 129–140. [CrossRef] [PubMed]

18. Marek, S.; Dosenbach, N.U.F. The frontoparietal network: Function, electrophysiology, and importance of individual precision mapping. *Dialog. Clin. Neurosci.* **2018**, *20*, 133–140.

19. Buschman, T.J.; Kastner, S. From Behavior to Neural Dynamics: An Integrated Theory of Attention. *Neuron* **2015**, *88*, 127–144. [CrossRef] [PubMed]

20. Safaai, H.; Neves, R.; Eschenko, O.; Logothetis, N.K.; Panzeri, S. Modeling the effect of locus coeruleus firing on cortical state dynamics and single-trial sensory processing. *Proc. Natl. Acad. Sci. USA* **2015**, *112*, 12834–12839. [CrossRef] [PubMed]

21. Bari, A.; Xu, S.; Pignatelli, M.; Takeuchi, D.; Feng, J.; Li, Y.; Tonegawa, S. Differential attentional control mechanisms by two distinct noradrenergic coeruleo-frontal cortical pathways. *Proc. Natl. Acad. Sci. USA* **2020**, *117*, 29080–29089. [CrossRef]

22. Lee, T.-H.; Greening, S.G.; Ueno, T.; Clewett, D.; Ponzio, A.; Sakaki, M.; Mather, M. Arousal increases neural gain via the locus coeruleus–noradrenaline system in younger adults but not in older adults. *Nat. Hum. Behav.* **2018**, *2*, 356–366. [CrossRef] [PubMed]

23. Vazey, E.M.; Moorman, D.E.; Aston-Jones, G. Phasic locus coeruleus activity regulates cortical encoding of salience information. *Proc. Natl. Acad. Sci. USA* **2018**, *115*, E9439–E9448. [CrossRef] [PubMed]

24. Mather, M.; Clewett, D.; Sakaki, M.; Harley, C.W. Norepinephrine ignites local hotspots of neuronal excitation: How arousal amplifies selectivity in perception and memory. *Behav. Brain Sci.* **2015**, *39*, E200. [CrossRef]

25. Berridge, C.W.; Waterhouse, B.D. The locus coeruleus–noradrenergic system: Modulation of behavioral state and state-dependent cognitive processes. *Brain Res. Rev.* **2003**, *42*, 33–84. [CrossRef]

26. Rodenkirch, C.; Liu, Y.; Schriver, B.J.; Wang, Q. Locus coeruleus activation enhances thalamic feature selectivity via norepinephrine regulation of intrathalamic circuit dynamics. *Nat. Neurosci.* **2018**, *22*, 120–133. [CrossRef] [PubMed]

27. Waschke, L.; Tune, S.; Obleser, J. Local cortical desynchronization and pupil-linked arousal differentially shape brain states for optimal sensory performance. *eLife* **2019**, *8*, e51501. [CrossRef]

28. Gelbard-Sagiv, H.; Magidov, E.; Sharon, H.; Hendler, T.; Nir, Y. Noradrenaline Modulates Visual Perception and Late Visually Evoked Activity. *Curr. Biol.* **2018**, *28*, 2239–2249.e6. [CrossRef]

29. Pfeffer, T.; Avramiea, A.-E.; Nolte, G.; Engel, A.K.; Linkenkaer-Hansen, K.; Donner, T.H. Catecholamines alter the intrinsic variability of cortical population activity and perception. *PLoS Biol.* **2018**, *16*, e2003453. [CrossRef]

30. Sharon, O.; Fahoum, F.; Nir, Y. Transcutaneous Vagus Nerve Stimulation in Humans Induces Pupil Dilation and Attenuates Alpha Oscillations. *J. Neurosci.* **2020**, *41*, 320–330. [CrossRef]

31. Pfeffer, T.; Ponce-Alvarez, A.; Tsetsos, K.; Meindertsma, T.; Gahnström, C.J.; Brink, R.L.V.D.; Nolte, G.; Engel, A.K.; Deco, G.; Donner, T.H. Circuit mechanisms for the chemical modulation of cortex-wide network interactions and behavioral variability. *Sci. Adv.* **2021**, *7*, eabf5620. [CrossRef]

32. Maier, S.U.; Grueschow, M. Pupil dilation predicts individual self-regulation success across domains. *Sci. Rep.* **2021**, *11*, 14342 . [CrossRef]

33. Kurniawan, I.T.; Grueschow, M.; Ruff, C.C. Anticipatory Energization Revealed by Pupil and Brain Activity Guides Human Effort-Based Decision Making. *J. Neurosci.* **2021**, *41*, 6328–6342. [CrossRef] [PubMed]

34. Grueschow, M.; Kleim, B.; Ruff, C.C. Role of the locus coeruleus arousal system in cognitive control. *J. Neuroendocr.* **2020**, *32*, e12890. [CrossRef] [PubMed]

35. Grueschow, M.; Stenz, N.; Thörn, H.; Ehlert, U.; Breckwoldt, J.; Maeder, M.B.; Exadaktylos, A.K.; Bingisser, R.; Ruff, C.C.; Kleim, B. Real-world stress resilience is associated with the responsivity of the locus coeruleus. *Nat. Commun.* **2021**, *12*, 2275. [CrossRef] [PubMed]

36. Köhler, S.; Bär, K.-J.; Wagner, G. Differential involvement of brainstem noradrenergic and midbrain dopaminergic nuclei in cognitive control. *Hum. Brain Mapp.* **2016**, *37*, 2305–2318. [CrossRef] [PubMed]

37. Köhler, S.; Wagner, G.; Bär, K. Activation of brainstem and midbrain nuclei during cognitive control in medicated patients with schizophrenia. *Hum. Brain Mapp.* **2018**, *40*, 202–213. [CrossRef] [PubMed]

38. Manger, P.R.; Eschenko, O. The Mammalian Locus Coeruleus Complex—Consistencies and Variances in Nuclear Organization. *Brain Sci.* **2021**, *11*, 1486. [CrossRef]

39. Berridge, C.W. Noradrenergic modulation of arousal. *Brain Res. Rev.* **2008**, *58*, 1–17. [CrossRef]

40. Poe, G.R.; Foote, S.; Eschenko, O.; Johansen, J.P.; Bouret, S.; Aston-Jones, G.; Harley, C.W.; Manahan-Vaughan, D.; Weinshenker, D.; Valentino, R.; et al. Locus coeruleus: A new look at the blue spot. *Nat. Rev. Neurosci.* **2020**, *21*, 644–659. [CrossRef]

41. McGinley, M.J.; Vinck, M.; Reimer, J.; Batista-Brito, R.; Zagha, E.; Cadwell, C.; Tolias, A.S.; Cardin, J.A.; McCormick, D.A. Waking State: Rapid Variations Modulate Neural and Behavioral Responses. *Neuron* **2015**, *87*, 1143–1161. [CrossRef]

42. McCormick, D.A.; Nestvogel, D.B.; He, B. Neuromodulation of Brain State and Behavior. *Annu. Rev. Neurosci.* **2020**, *43*, 391–415. [CrossRef] [PubMed]

43. Reimer, J.; Froudarakis, E.; Cadwell, C.; Yatsenko, D.; Denfield, G.H.; Tolias, A.S. Pupil Fluctuations Track Fast Switching of Cortical States during Quiet Wakefulness. *Neuron* **2014**, *84*, 355–362. [CrossRef]

44. Zerbi, V.; Floriou-Servou, A.; Markicevic, M.; Vermeiren, Y.; Sturman, O.; Privitera, M.; von Ziegler, L.; Ferrari, K.D.; Weber, B.; De Deyn, P.P.; et al. Rapid Reconfiguration of the Functional Connectome after Chemogenetic Locus Coeruleus Activation. *Neuron* **2019**, *103*, 702–718.e5. [CrossRef] [PubMed]

45. Carter, M.; Yizhar, O.; Chikahisa, S.; Nguyen, H.; Adamantidis, A.; Nishino, S.; Deisseroth, K.; De Lecea, L. Tuning arousal with optogenetic modulation of locus coeruleus neurons. *Nat. Neurosci.* **2010**, *13*, 1526–1533. [CrossRef] [PubMed]

46. Aston-Jones, G. Locus Coeruleus, A5 and A7 Noradrenergic Cell Groups. In *The Rat Nervous System*, 3rd ed.; Paxinos, G., Ed.; Academic Press: Cambridge, MA, USA, 2004; pp. 259–294. [CrossRef]

47. Pickel, V.M.; Segal, M.; Bloom, F.E. A radioautographic study of the efferent pathways of the nucleus locus coeruleus. *J. Comp. Neurol.* **1974**, *155*, 15–41. [CrossRef]

48. Jones, B.E.; Moore, R.Y. Ascending projections of the locus coeruleus in the rat. II. Autoradiographic study. *Brain Res.* **1977**, *127*, 25–53. [CrossRef]

49. Nomura, S.; Bouhadana, M.; Morel, C.; Faure, P.; Cauli, B.; Lambolez, B.; Hepp, R.; Hepp, R. Noradrenalin and dopamine receptors both control cAMP-PKA signaling throughout the cerebral cortex. *Front. Cell. Neurosci.* **2014**, *8*, 247. [CrossRef]

50. Berridge, C.W.; Stratford, T.L.; Foote, S.L.; Kelley, A.E. Distribution of dopamine beta-hydroxylase-like immunoreactive fibers within the shell subregion of the nucleus accumbens. *Synapse* **1997**, *27*, 230–241. [CrossRef]

51. Schroeter, S.; Apparsundaram, S.; Wiley, R.G.; Miner, L.H.; Sesack, S.R.; Blakely, R.D. Immunolocalization of the cocaine- and antidepressant-sensitive l-norepinephrine transporter. *J. Comp. Neurol.* **2000**, *420*, 211–232. [CrossRef]

52. Verguts, T.; Notebaert, W. Hebbian learning of cognitive control: Dealing with specific and nonspecific adaptation. *Psychol. Rev.* **2008**, *115*, 518–525. [CrossRef]

53. Notebaert, W.; Verguts, T. Cognitive control acts locally. *Cognition* **2008**, *106*, 1071–1080. [CrossRef] [PubMed]

54. Joshi, S.; Li, Y.; Kalwani, R.M.; Gold, J.I. Relationships between Pupil Diameter and Neuronal Activity in the Locus Coeruleus, Colliculi, and Cingulate Cortex. *Neuron* **2015**, *89*, 221–234. [CrossRef] [PubMed]

55. Joshi, S.; Gold, J.I. Pupil Size as a Window on Neural Substrates of Cognition. *Trends Cogn. Sci.* **2020**, *24*, 466–480. [CrossRef] [PubMed]

56. Liu, Y.; Rodenkirch, C.; Moskowitz, N.; Schriver, B.; Wang, Q. Dynamic Lateralization of Pupil Dilation Evoked by Locus Coeruleus Activation Results from Sympathetic, Not Parasympathetic, Contributions. *Cell Rep.* **2017**, *20*, 3099–3112. [CrossRef] [PubMed]

57. Reimer, J.; McGinley, M.J.; Liu, Y.; Rodenkirch, C.; Wang, Q.; McCormick, D.A.; Tolias, A.S. Pupil fluctuations track rapid changes in adrenergic and cholinergic activity in cortex. *Nat. Commun.* **2016**, *7*, 13289. [CrossRef] [PubMed]

58. Murphy, P.R.; O'Connell, R.G.; O'Sullivan, M.; Robertson, I.H.; Balsters, J.H. Pupil diameter covaries with BOLD activity in human locus coeruleus. *Hum. Brain Mapp.* **2014**, *35*, 4140–4154. [CrossRef] [PubMed]

59. De Gee, J.W.; Colizoli, O.; Kloosterman, N.A.; Knapen, T.; Nieuwenhuis, S.; Donner, T.H. Dynamic modulation of decision biases by brainstem arousal systems. *eLife* **2017**, *6*, e23232. [CrossRef]

60. Unsworth, N.; Robison, M.K. A locus coeruleus-norepinephrine account of individual differences in working memory capacity and attention control. *Psychon. Bull. Rev.* **2017**, *24*, 1282–1311. [CrossRef]

61. Unsworth, N.; Robison, M.K. The importance of arousal for variation in working memory capacity and attention control: A latent variable pupillometry study. *J. Exp. Psychol. Learn. Mem. Cogn.* **2017**, *43*, 1962–1987. [CrossRef]

62. Manohar, S.G.; Chong, T.; Apps, M.; Batla, A.; Stamelou, M.; Jarman, P.R.; Bhatia, K.P.; Husain, M. Reward Pays the Cost of Noise Reduction in Motor and Cognitive Control. *Curr. Biol.* **2015**, *25*, 1707–1716. [CrossRef]

63. Heitz, R.P. The speed-accuracy tradeoff: History, physiology, methodology, and behavior. *Front. Neurosci.* **2014**, *8*, 150. [CrossRef] [PubMed]

64. Polania, R.; Krajbich, I.; Grueschow, M.; Ruff, C. Neural Oscillations and Synchronization Differentially Support Evidence Accumulation in Perceptual and Value-Based Decision Making. *Neuron* **2014**, *82*, 709–720. [CrossRef] [PubMed]

65. Robinson, E.; Eagle, D.; Mar, A.C.; Bari, A.; Banerjee, G.; Jiang, X.; Dalley, J.; Robbins, T. Similar Effects of the Selective Noradrenaline Reuptake Inhibitor Atomoxetine on Three Distinct Forms of Impulsivity in the Rat. *Neuropsychopharmacology* **2007**, *33*, 1028–1037. [CrossRef] [PubMed]

66. Bari, A.; Mar, A.C.; Theobald, D.E.; Elands, S.A.; Oganya, K.C.N.A.; Eagle, D.M.; Robbins, T.W. Prefrontal and Monoaminergic Contributions to Stop-Signal Task Performance in Rats. *J. Neurosci.* **2011**, *31*, 9254–9263. [CrossRef]

67. Pattij, T.; Schetters, D.; Schoffelmeer, A.N.M.; Van Gaalen, M.M. On the improvement of inhibitory response control and visuospatial attention by indirect and direct adrenoceptor agonists. *Psychopharmacology* **2011**, *219*, 327–340. [CrossRef]

68. Navarra, R.; Graf, R.; Huang, Y.; Logue, S.; Comery, T.; Hughes, Z.; Day, M. Effects of atomoxetine and methylphenidate on attention and impulsivity in the 5-choice serial reaction time test. *Prog. Neuro-Psychopharmacology Biol. Psychiatry* **2008**, *32*, 34–41. [CrossRef]

69. Bari, A.; Robbins, T.W. Noradrenergic versus dopaminergic modulation of impulsivity, attention and monitoring behaviour in rats performing the stop-signal task. *Psychopharmacology* **2013**, *230*, 89–111. [CrossRef]

70. Etkin, A.; Egner, T.; Peraza, D.M.; Kandel, E.R.; Hirsch, J. Resolving Emotional Conflict: A Role for the Rostral Anterior Cingulate Cortex in Modulating Activity in the Amygdala. *Neuron* **2006**, *51*, 871–882. [CrossRef]

71. Egner, T.; Etkin, A.; Gale, S.; Hirsch, J. Dissociable Neural Systems Resolve Conflict from Emotional versus Nonemotional Distracters. *Cereb. Cortex* **2007**, *18*, 1475–1484. [CrossRef]

72. Robinson, O.J.; Letkiewicz, A.; Overstreet, C.; Ernst, M.; Grillon, C. The effect of induced anxiety on cognition: Threat of shock enhances aversive processing in healthy individuals. *Cogn. Affect. Behav. Neurosci.* **2011**, *11*, 217–227. [CrossRef]

73. Braem, S.; King, J.; Korb, F.; Krebs, R.M.; Notebaert, W.; Egner, T. The Role of Anterior Cingulate Cortex in the Affective Evaluation of Conflict. *J. Cogn. Neurosci.* **2017**, *29*, 137–149. [CrossRef] [PubMed]

74. Dreisbach, G.; Fischer, R. Conflicts as Aversive Signals for Control Adaptation. *Curr. Dir. Psychol. Sci.* **2015**, *24*, 255–260. [CrossRef]

75. Egner, T. Congruency sequence effects and cognitive control. *Cogn. Affect. Behav. Neurosci.* **2007**, *7*, 380–390. [CrossRef] [PubMed]

76. Monti, J.M.; Weintraub, S.; Egner, T. Differential age-related decline in conflict-driven task-set shielding from emotional versus non-emotional distracters. *Neuropsychologia* **2010**, *48*, 1697–1706. [CrossRef]

77. Keren, N.I.; Lozar, C.T.; Harris, K.; Morgan, P.; Eckert, M.A. In vivo mapping of the human locus coeruleus. *NeuroImage* **2009**, *47*, 1261–1267. [CrossRef]

78. Ashburner, J.; Friston, K. Unified segmentation. *NeuroImage* **2005**, *26*, 839–851. [CrossRef]

79. Dimigen, O.; Valsecchi, M.; Sommer, W.; Kliegl, R. Human Microsaccade-Related Visual Brain Responses. *J. Neurosci.* **2009**, *29*, 12321–12331. [CrossRef]

80. Tse, P.U.; Baumgartner, F.J.; Greenlee, M.W. Event-related functional MRI of cortical activity evoked by microsaccades, small visually-guided saccades, and eyeblinks in human visual cortex. *NeuroImage* **2010**, *49*, 805–816. [CrossRef]

81. Grueschow, M.; Polania, R.; Hare, T.; Ruff, C.C. Automatic versus Choice-Dependent Value Representations in the Human Brain. *Neuron* **2015**, *85*, 874–885. [CrossRef]

82. Schumann, A.; Köhler, S.; de la Cruz, F.; Güllmar, D.; Reichenbach, J.R.; Wagner, G.; Bär, K.-J. The Use of Physiological Signals in Brainstem/Midbrain fMRI. *Front. Neurosci.* **2018**, *12*, 718. [CrossRef]

83. Bazin, P.-L.; Alkemade, A.; van der Zwaag, W.; Caan, M.W.; Mulder, M.; Forstmann, B.U. Denoising High-Field Multi-Dimensional MRI With Local Complex PCA. *Front. Neurosci.* **2019**, *13*, 1066. [CrossRef] [PubMed]

84. Nichols, T.E.; Holmes, A.P. Nonparametric permutation tests for functional neuroimaging: A primer with examples. *Hum. Brain Mapp.* **2002**, *15*, 1–25. [CrossRef] [PubMed]

85. Kerns, J.G.; Cohen, J.D.; MacDonald, A.W.; Cho, R.Y.; Stenger, V.A.; Carter, C.S. Anterior Cingulate Conflict Monitoring and Adjustments in Control. *Science* **2004**, *303*, 1023–1026. [CrossRef] [PubMed]

86. Liu, K.Y.; Marijatta, F.; Hämmerer, D.; Acosta-Cabronero, J.; Düzel, E.; Howard, R.J. Magnetic resonance imaging of the human locus coeruleus: A systematic review. *Neurosci. Biobehav. Rev.* **2017**, *83*, 325–355. [CrossRef] [PubMed]

87. Chamberlain, S.R.; Robbins, T. Noradrenergic modulation of cognition: Therapeutic implications. *J. Psychopharmacol.* **2013**, *27*, 694–718. [CrossRef]

88. Chamberlain, S.R.; Muller, U.; Blackwell, A.D.; Clark, L.; Robbins, T.W.; Sahakian, B.J. Neurochemical Modulation of Response Inhibition and Probabilistic Learning in Humans. *Science* **2006**, *311*, 861–863. [CrossRef]

89. Schwarz, L.A.; Miyamichi, K.; Gao, X.J.; Beier, K.T.; Weissbourd, B.; Deloach, K.E.; Ren, J.; Ibanes, S.; Malenka, R.C.; Kremer, E.J.; et al. Viral-genetic tracing of the input–output organization of a central noradrenaline circuit. *Nature* **2015**, *524*, 88–92. [CrossRef]

90. Arnsten, A.; Goldman-Rakic, P. Selective prefrontal cortical projections to the region of the locus coeruleus and raphe nuclei in the rhesus monkey. *Brain Res.* **1984**, *306*, 9–18. [CrossRef]

91. Porrino, L.J.; Goldman-Rakic, P.S. Brainstem innervation of prefrontal and anterior cingulate cortex in the rhesus monkey revealed by retrograde transport of HRP. *J. Comp. Neurol.* **1982**, *205*, 63–76. [CrossRef]

92. Tervo, D.G.; Proskurin, M.; Manakov, M.; Kabra, M.; Vollmer, A.; Branson, K.; Karpova, A.Y. Behavioral Variability through Stochastic Choice and Its Gating by Anterior Cingulate Cortex. *Cell* **2014**, *159*, 21–32. [CrossRef]

93. Chandler, D.J.; Waterhouse, B.D.; Gao, W.-J. New perspectives on catecholaminergic regulation of executive circuits: Evidence for independent modulation of prefrontal functions by midbrain dopaminergic and noradrenergic neurons. *Front. Neural Circuits* **2014**, *8*, 53. [CrossRef] [PubMed]

94. Waterhouse, B.; Chandler, D.; Prouty, E.; Gao, W.J. Electrophysiological Properties of Locus Coeruleus-Prefrontal Cortical Projection Neurons in Normal and Inattentive Rats. *Neuropsychopharmacol* **2014**, *39*, S167.

95. Chandler, D.J.; Gao, W.-J.; Waterhouse, B.D. Heterogeneous organization of the locus coeruleus projections to prefrontal and motor cortices. *Proc. Natl. Acad. Sci. USA* **2014**, *111*, 6816–6821. [CrossRef] [PubMed]

96. Redmond, D.; Huang, Y., II. New evidence for a locus coeruleus-norepinephrine connection with anxiety. *Life Sci.* **1979**, *25*, 2149–2162. [CrossRef]

97. Weiss, J.M.; Stout, J.; Aaron, M.F.; Quan, N.; Owens, M.J.; Butler, P.D.; Nemeroff, C.B. Depression and anxiety: Role of the locus coeruleus and corticotropin-releasing factor. *Brain Res. Bull.* **1994**, *35*, 561–572. [CrossRef]

98. Itoi, K.; Sugimoto, N. The Brainstem Noradrenergic Systems in Stress, Anxiety and Depression. *J. Neuroendocr.* **2010**, *22*, 355–361. [CrossRef]

99. McCall, J.G.; Siuda, E.R.; Bhatti, D.L.; Lawson, L.A.; McElligott, Z.A.; Stuber, G.D.; Bruchas, M.R. Locus coeruleus to basolateral amygdala noradrenergic projections promote anxiety-like behavior. *eLife* **2017**, *6*, e18247. [CrossRef]

100. Tanaka, M.; Yoshida, M.; Emoto, H.; Ishii, H. Noradrenaline systems in the hypothalamus, amygdala and locus coeruleus are involved in the provocation of anxiety: Basic studies. *Eur. J. Pharmacol.* **2000**, *405*, 397–406. [CrossRef]

101. Zhu, M.-Y.; Klimek, V.; Dilley, G.E.; Haycock, J.W.; Stockmeier, C.; Overholser, J.C.; Meltzer, H.Y.; Ordway, G.A. Elevated levels of tyrosine hydroxylase in the locus coeruleus in major depression. *Biol. Psychiatry* **1999**, *46*, 1275–1286. [CrossRef]

102. Naegeli, C.; Zeffiro, T.; Piccirelli, M.; Jaillard, A.; Weilenmann, A.; Hassanpour, K.; Schick, M.; Rufer, M.; Orr, S.P.; Mueller-Pfeiffer, C. Locus Coeruleus Activity Mediates Hyperresponsiveness in Posttraumatic Stress Disorder. *Biol. Psychiatry* **2018**, *83*, 254–262. [CrossRef]

103. Southwick, S.M.; Bremner, J.D.; Rasmusson, A.; Morgan, C.A.; Arnsten, A.; Charney, D.S. Role of norepinephrine in the pathophysiology and treatment of posttraumatic stress disorder. *Biol. Psychiatry* **1999**, *46*, 1192–1204. [CrossRef]

104. Grueschow, M.; Jelezarova, I.; Westphal, M.; Ehlert, U.; Kleim, B. Emotional conflict adaptation predicts intrusive memories. *PLoS ONE* **2020**, *15*, e0225573. [CrossRef] [PubMed]

105. McCall, J.G.; Al-Hasani, R.; Siuda, E.R.; Hong, D.Y.; Norris, A.; Ford, C.P.; Bruchas, M.R. CRH Engagement of the Locus Coeruleus Noradrenergic System Mediates Stress-Induced Anxiety. *Neuron* **2015**, *87*, 605–620. [CrossRef] [PubMed]

106. Ju, H.; Bassett, D.S. Dynamic representations in networked neural systems. *Nat. Neurosci.* **2020**, *23*, 908–917. [CrossRef] [PubMed]

107. Schmitt, F.; Kaufmann, J.; Hoffmann, M.; Tempelmann, C.; Kluge, C.; Rampp, S.; Voges, J.; Heinze, H.; Buentjen, L.; Grueschow, M. Case Report: Practicability of functionally based tractography of the optic radiation during presurgical epilepsy work up. *Neurosci. Lett.* **2014**, *568*, 56–61. [CrossRef]

108. Loewe, K.; Grueschow, M.; Stoppel, C.M.; Kruse, R.; Borgelt, C. Fast construction of voxel-level functional connectivity graphs. *BMC Neurosci.* **2014**, *15*, 78. [CrossRef] [PubMed]

109. Bassett, D.S.; Zurn, P.; Gold, J.I. On the nature and use of models in network neuroscience. *Nat. Rev. Neurosci.* **2018**, *19*, 566–578. [CrossRef] [PubMed]

110. Brown, G.G.; Kindermann, S.S.; Siegle, G.J.; Granholm, E.; Wong, E.C.; Buxton, R.B. Brain activation and pupil response during covert performance of the Stroop Color Word task. *J. Int. Neuropsychol. Soc.* **1999**, *5*, 308–319. [CrossRef]

111. Siegle, G.J.; Steinhauer, S.; Thase, M.E. Pupillary assessment and computational modeling of the Stroop task in depression. *Int. J. Psychophysiol.* **2004**, *52*, 63–76. [CrossRef]

112. Siegle, G.J.; Ichikawa, N.; Steinhauer, S. Blink before and after you think: Blinks occur prior to and following cognitive load indexed by pupillary responses. *Psychophysiology* **2008**, *45*, 679–687. [CrossRef]

113. Laeng, B.; Ørbo, M.; Holmlund, T.; Miozzo, M. Pupillary Stroop effects. *Cogn. Process.* **2010**, *12*, 13–21. [CrossRef] [PubMed]

114. Van Der Wel, P.; Van Steenbergen, H. Pupil dilation as an index of effort in cognitive control tasks: A review. *Psychon. Bull. Rev.* **2018**, *25*, 2005–2015. [CrossRef] [PubMed]

115. Saposnik, G.; Grueschow, M.; Oh, J.; Terzaghi, M.A.; Kostyrko, P.; Vaidyanathan, S.; Nisenbaum, R.; Ruff, C.C.; Tobler, P.N. Effect of an Educational Intervention on Therapeutic Inertia in Neurologists with Expertise in Multiple Sclerosis. *JAMA Netw. Open* **2020**, *3*, e2022227. [CrossRef] [PubMed]

116. Azza, Y.; Grueschow, M.; Karlen, W.; Seifritz, E.; Kleim, B. How stress affects sleep and mental health: Nocturnal heart rate increases during prolonged stress and interacts with childhood trauma exposure to predict anxiety. *Sleep* **2019**, *43*, zsz310. [CrossRef] [PubMed]

117. Maier, S.U.; Makwana, A.B.; Hare, T.A. Acute Stress Impairs Self-Control in Goal-Directed Choice by Altering Multiple Functional Connections within the Brain's Decision Circuits. *Neuron* **2015**, *87*, 621–631. [CrossRef]

118. Boden, J.M.; McLeod, G.F.H. Resilience and psychiatric epidemiology: Implications for a conceptual framework. *Behav. Brain Sci.* **2015**, *38*, e95. [CrossRef] [PubMed]

119. Pitman, R.K.; Rasmusson, A.M.; Koenen, K.; Shin, L.M.; Orr, S.P.; Gilbertson, M.W.; Milad, M.R.; Liberzon, I. Biological studies of post-traumatic stress disorder. *Nat. Rev. Neurosci.* **2012**, *13*, 769–787. [CrossRef]

120. Ruscio, A.M.; Hallion, L.S.; Lim, C.C.W.; Aguilar-Gaxiola, S.; Al-Hamzawi, A.; Alonso, J.; Andrade, L.H.; Borges, G.; Bromet, E.J.; Bunting, B.; et al. Cross-sectional Comparison of the Epidemiology of DSM-5 Generalized Anxiety Disorder Across the Globe. *JAMA Psychiatry* **2017**, *74*, 465–475. [CrossRef]